International Journal of Environmental Science and Technology (2026) 23:99
https://doi.org/10.1007/s13762-025-06878-4

ORIGINAL PAPER

Effect of traffic density on heavy metal content of forest trees in chessmaster park in Astana, Kazakhstan

S. Ayan[1] · D. Sarsekova[2] · G. Kenesaryuly[3] · G. Savaci Selamet[4] · O. Gülseven[5] · E. Yilmaz[5,6] · S. S. Akin[5]

Received: 24 August 2024 / Revised: 16 September 2025 / Accepted: 30 September 2025 / Published online: 4 December 2025

Abstract
The study investigates the changes in heavy metal concentrations in the leaves of urban trees in Chessmaster Park in Astana, Kazakhstan. Samples were collected from areas located 10–15 m from the main road (high pollution), 15–30 m from the secondary road (moderate pollution), and 30–80 m from the non-road (low pollution). Air pollution data for 2020 and 2021 was sourced from Kazhydromet, and graphs were created. The findings indicate that traffic-related pollution has led to significant variations in the accumulation of most heavy metals, except for manganese, nickel, and zinc. In areas of light and moderate pollution where *Betula pendula* was present, higher concentrations of zinc (197.488 and 481.275 mg kg^{-1}), and manganese (163.07 and 157.741 mg kg^{-1}) were observed, while lead (3.123 mg kg^{-1}) was found in higher concentrations in the moderate pollution zones. Silver concentrations were notably higher in all tree species across all traffic pollution levels. Aluminum and iron deficiencies were observed in all pollution zones, particularly in *Betula pendula* and *Picea pungens*. The results also revealed extremely high levels of $PM_{2.5}$ and PM_{10} in 2021, with mean concentrations of 50.7 µg m^{-3} and 130 µg m^{-3}, respectively, exceeding the limit values. Additionally, heavy metal accumulation in urban trees was found to be influenced by air quality, traffic density, and silver toxicity, especially when tree roots were exposed to sewage. Overall, these results highlight the accumulation of heavy metals from groundwater, air pollution, traffic emissions, and other human activities.

Keywords Anthropogenic factors · Traffic-related pollution · Tree species · Urban roadside park

Introduction

According to the World Bank's Collection of Development Indicators (WDB 2025), around 57% of the world's population lived in urban areas in 2023. In Kazakhstan, the urbanization rate was projected to reach up to 63% by the end

Editorial responsibility: Samareh Mirkia.

✉ G. Savaci Selamet
gsavaci@kastamonu.edu.tr

S. Ayan
sezginayan@gmail.com

D. Sarsekova
dani999@mail.ru

G. Kenesaryuly
ganion@inbox.ru

O. Gülseven
orhan.gulseven@hotmail.com

E. Yilmaz
yilmazergin1982@gmail.com

S. S. Akin
selinalptekin02@gmail.com

1 Faculty of Forestry, Silviculture Department, Kastamonu University, Kastamonu, Türkiye

2 The Faculty of Forestry and Land Resources, Kazakh National Agrarian Research University, Almaty, Kazakhstan

3 Institute of Agriculture and Forestry, S. Seifullin Kazakh Agrotechnical Research University, Astana, Kazakhstan

4 Faculty of Forestry, Department of Soil Science and Ecology, Kastamonu University, Kastamonu, Türkiye

5 Institute of Science, Sustainable Forestry Doct. Programme, Kastamonu University, Kastamonu, Türkiye

6 The Union of Chambers and Commodity Exchanges of Türkiye-Devrekâni Vocational High School, Kastamonu University, Devrekâni, Kastamonu, Türkiye

of 2024, with an urban population of roughly 12 million, marking an 8% increase since 2017 (BUREAU of National Statistics 2025). Vehicular traffic, a major contributor to heavy metal pollution in urban areas and roadside dust, has increased in recent years due to population growth and urbanization (Heidari et al. 2021; Kumar et al. 2021). Astana currently has about 309 thousand vehicles (Ayan et al. 2021). Metal pollution, primarily from traffic-related exhaust emissions, decreases as the distance from major roads increases (Dao et al. 2014; Huang et al. 2021; Wang et al. 2022) and is closely associated with the traffic density on nearby roads (Wang et al. 2018; Huang et al. 2021). For instance, Kumar et al. (2025) noted that concentrations of Cr, Co, Zn, Pb, Ni, and Cu caused by vehicle emissions along the National Highway and State Highway roadside soils in Haryana, whereas the local route and highway roadside soils showed a further declining trend.

Traffic-related pollution, a major contributor to air pollution (Ghio et al. 2012; Costa et al. 2019), continues to intensify due to the increasing number of vehicles as a result of changing living standards and rapid population growth. Air pollutants such as particulate matter (PM) and nitrogen dioxide (NO_2) are among the most important components of traffic emissions. PM produced by the combustion of fossil fuels in vehicles and the resuspension of road dust can lead to deterioration of air quality and have a significant negative impact on the health of the urban population (Jin et al. 2014). Emissions from vehicles have been found to be a major concern for the tree species in the area and the nearby population (Singh et al. 2020). However, trees and shrubs in urban parks, which are planned as important elements of urban green spaces, can act as air filters to reduce pollution to some extent. Trees in urban areas, particularly in traffic-exposed spaces, play a beneficial role in reducing pollution, with a 10-m-wide green belt capable of decreasing pollution levels by up to 50% (Kończak et al. 2021). Futhermore, with rapid urbanization, urban parks play a critical role in maintaining ecological balance within urban environments (Coulon et al. 2016). The urban parks consist of various tree species that can effectively mitigate the effects of air pollution from vehicles, thereby alleviating the major problem of air pollution (Singh et al. 2020). Urban parks are typically located adjacent to main roads, making them suitable locations for investigating the effects of spatial metal pollution caused by traffic-related exhaust emissions (Zhao et al. 2020; Wang et al. 2022). Chessmaster urban park, located at the end of a highway with active and heavy traffic in Astana, has become an important site for public recreation.

According to the 2020 census, Astana has a population of 1.1 million (Almaganbetovna et al. 2023). Due to its unique climatic conditions, such as extensive sandy and clay desert areas, scarce vegetation, and frequent storms, the city experiences sand and dust storm events (Orlovsky et al. 2013; Issanova et al. 2023), resulting in severe exposure to gaseous and particulate air pollution. In addition, the rapid increase in the number of motor vehicles in recent years has resulted in high levels of traffic pollution, which has been identified as one of the main factors contributing to the deterioration of the city's environmental quality. Therefore, there is an urgent need for detailed studies to assess the potential impacts of traffic pollution on urban plant systems. To fill this gap, it is necessary to identify heavy metals in tree species of Chessmaster Park, which is of great importance in Astana, and to evaluate the possible effects of different traffic densities on the health of urban park trees. This study was conducted in November 2020 and aimed to investigate the effects of heavy metals (Ni, Cd, Mn, Pb, Cr, Li, Co, Fe, Pb, Ba, Ag, Zn, etc.) on six tree species viz., *Picea abies* (L.) H. Karst., *Picea pungens* Engelm., *Pinus sylvestris* L., *Juniperus* sp., *Larix* sp., and *Betula pendula* Roth exposed to different levels of traffic pollutants in the Chessmaster Park of Astana, the capital of Kazakhstan.

Materials and methods

Study area

The study was conducted in Chessmaster Park, located at 51°09′53" north latitude and 71°23′35" east longitude, near roads of varying traffic density in Astana, the capital city of Kazakhstan (Fig. 1). Astana is located in central Kazakhstan along the Ishim River, in a flat, semi-arid steppe region, at an elevation of 347 m above sea level.

Astana, the second-largest city in Kazakhstan, is expanding its city limits due to increasing population density. For landscaping in the city's parks, tree species that are highly resistant to the harsh continental climate are commonly used. This study focuses on deciduous and coniferous forest tree species growing in Chessmaster Park, including species from the Betulaceae family such as *B. pendula*; the Pinaceae family such as *P. sylvestris, P. pungens, P. abies, and Larix* sp., and the Cupressaceae family such as *Juniperus* sp. The study examines different levels of pollution: i) High pollution (HP) refers to sample plots 1, 2, 3, 4, and 9, located in the eastern part of Chessmaster Park, approximately 10–15 m from the two-way Republic Avenue expressway (main road) with heavy urban traffic. ii) Moderate Pollution (MP) refers to sample plots 8, 11, 12, 13, 19, 20, 22, 23, and 24 located in the northern part of Chessmaster Park, approximately 15–30 m from the one-way Kenesay Street (side road) with moderate traffic in the city. iii) Light

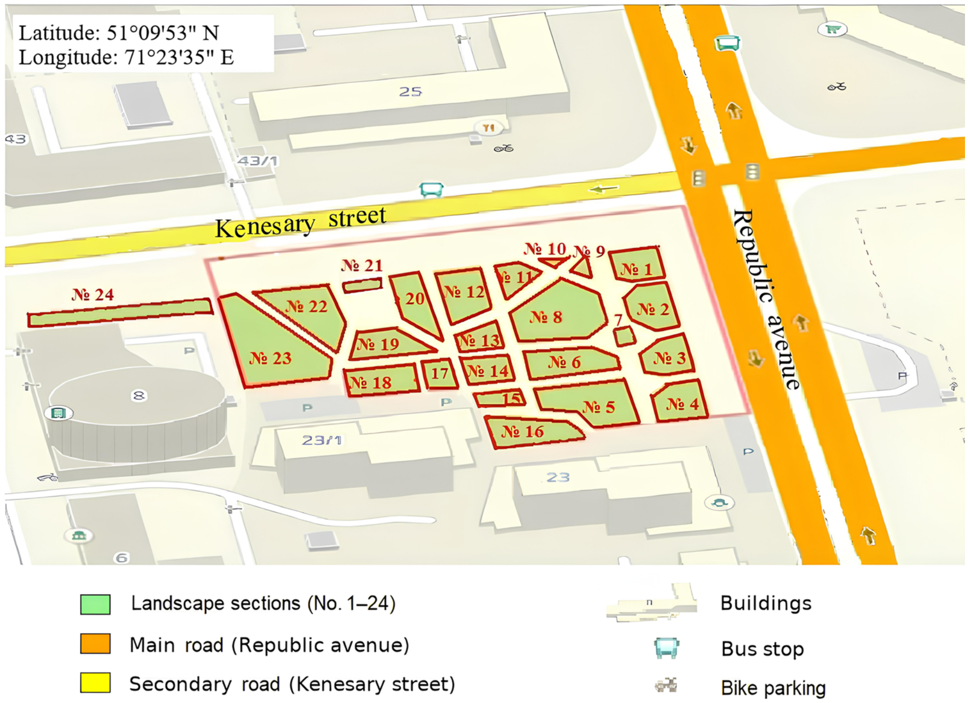

Fig. 1 The location of Chessmaster Park according to main and secondary roads

Table 1 Tree species in different plots of Chessmaster Park exposed to different levels of pollution

Exposure level of pollution	Chessmaster Park		
	Plot no	Distance from road (m)	Tree species
High	1	Main road 10–15 m	*P. abies, B. pendula*
	2		*P. abies, B. pendula*
	3		*P. abies, P. pungens, B. pendula*
	4		*P. abies, B. pendula*
	9		*P. abies*
Moderate	8	Side road 15–30 m	*P. abies, Larix* sp.
	11		*P. abies*
	12		*P. sylvestris*
	13		*P. abies*
	19		*Juniperus* sp., *P. abies*
	20		*B. pendula*
	22		*B. pendula, P. abies*
	23		*P. pungens*
	24		*P. abies, P. sylvestris*
Light	5	Areas not adjacent to any road 30–80 m	*P. pungens, P. abies, B. pendula*
	6		*P. abies, P. pungens*
	15		*P. abies*
	16		*P. abies, B. pendula*

Pollution (LP) refers to sample plots 5, 6, 15 and 16 which are located in the southern part of Chessmaster Park and are not adjacent to any road. Table 1 and Fig. 1 display the names and locations of the tree species at varying distances from the traffic roads surrounding Chessmaster Park. In the park, *P. abies*, *P. pungens*, and *B. pendula* species are found in areas exposed to three all levels of pollution, respectively. Therefore, these three species were evaluated based on their distance from pollution sources and their element accumulation status. *Juniperus* sp., *P. sylvestris*, and *Larix* sp. are found only in the moderate pollution areas. These pollution levels result from different traffic densities affecting *P. abies*,

Fig. 2 View of the Chessmaster Park

P. pungens, *P. sylvestris*, *Juniperus* sp., *Larix* sp., and *B. pendula* (Table 1 and Fig. 2).

Astana is the second coldest national capital in the world, characterized by an extreme continental climate with warm summers and long, very cold, dry winters. Summer temperatures can occasionally rise to 35 °C, while winter temperatures typically range between –30 °C and –35 °C from mid-December to early March. The average annual temperature is 3.1 °C, and the city receives 300 mm of precipitation annually (URL1 2021; Ayan et al. 2021). Strong winds are common in Astana, especially in the rapidly developing but relatively exposed northern parts of the city.

Leaf sampling and analysis

The analysis focused on leaves due to their high levels of heavy metal accumulation, as noted in previous studies (Hu et al. 2014; Matin et al. 2016). Leaf sampling was conducted in November 2020. Leaf samples were collected at the end of the vegetative period and transported to Kastamonu University's Central Research Laboratory for the analysis of heavy metals, including Ni, Cd, Pb, Cr, Li, Co, Fe, Mn, Al, Ba, Ag, and Zn. The samples were categorized based on tree species and their distance from the pollution source. To preserve the integrity of the samples for research purposes, they were neither washed nor wiped. The samples were labeled, air-dried for 15 days, and subsequently oven-dried at 45 °C until completely dry.

Next, the plant samples were ground to powder, and 0.5 g were weighed and placed in tubes designed for the MILESTONE MARS 6240–50 model microwave oven. Each sample was treated with 10 ml of 65% HNO_3 and then heated in a microwave at 280 PSI pressure and 180 °C for 20 min. After cooling, the samples were diluted to 50 ml with deionized water, filtered through filter paper, and analyzed using the Spectroblue II ICP-OES device. The detection limits for heavy metals using the ICP-OES device were as follows: Pb, 0.377 ppb; Cd, 0.063 ppb; Cr, 0.311 ppb; Ni, 0.171 ppb; Fe, 0.00068 mg kg^{-1}, and Zn, 0.00634 mg kg^{-1}. Normal range of heavy metal contents in plants is given in Table 2, and the results of leaf analysis were compared with these values. To determine the accuracy, Standard Reference Material (SRM) 1575a (NIST) (Sigma-Aldrich) was prepared and analyzed in triplicate in the same manner as the samples. For heavy metals, the calibration curve was established in the interval 1–100 mg L^{-1} (Merck, Milan, IT) and the amount of the minerals was expressed in mg g^{-1} dw.

Table 2 Reference ranges of heavy metal concentrations in plants

Heavy metals	Reference range in plants (mg kg^{-1})	Reference
Fe	640–2486	(Lavilla et al. 1999)
Mn	15–100	(Misra and Mani 1991)
Cr	0.006–18	(Zayed and Terry 2003)
Co	0.1–10	(Palit et al. 1994)
Ni	0.1–3.7	(Kabata-Pendias and Pendias 1984)
Pb	3	(Codex 2003)
Al	200	(Jansen et al. 2002)
Ba	< 200	(Pais and Jones 1997)
Cd	2	(FAO 2014)
Li	0.2–30	(Bolan et al. 2021)
Ag	0.01	(Kabata-Pendias and Pendias 2001)
Zn	1–160	(Abdel-Sabour and Rabie 2003)

Obtaining and ınterpreting air pollutant concentrations

Between January 1, 2020 and December 31, 2021, data on air pollutant concentrations ($PM_{2.5}$, PM_{10}, SO_2, and NO_2) were obtained from the official website of the Republican State Enterprise Kazhydromet (Kazhydromet 2024). These values were subsequently compared with the air quality limits established by the World Health Organization (2021). The World Health Organization's (2021) threshold values for the four primary pollutants are are given in Table 3.

Statistical evaluation

Variance analysis was performed for each variable based on the distance from the pollution source and the tree species, utilizing triplicate data obtained from the ICP-OES analysis. When significant differences were identified, the Newman-Keuls Multiple Test was applied to determine which tree species exhibited higher levels of heavy metal accumulation.

Results and discussion

Air pollution levels

The time series of monthly average concentrations of 4 air pollutants ($PM_{2.5}$, PM_{10}, SO_2, and NO_2) in Chessmaster Park in 2020 and 2021 are shown in Fig. 3. The $PM_{2.5}$ concentration showed a large temporal variability, with the highest concentration in winter (highest in January) in 2021, and relatively lower concentration in other months (Fig. 3a). The annual average of $PM_{2.5}$ was 30.8 µg m^{-3} in 2020 and 50.7 µg m^{-3} in 2021. According to the World Health Organization (2021), the limit value for $PM_{2.5}$ concentration is 10 µg m^{-3} per year. Accordingly, it can be seen that the averages of 2020 and 2021 exceeded the limit values and are about 3 to 5 times higher than this limit value (Fig. 3a). The annual average of $PM_{2.5}$ in Astana in 2020 is similar to that in Poland (30 µg m^{-3}) and Slovakia (31 µg m^{-3}) (Nadgórska-Socha et al. 2017) and much lower than that

Table 3 Air pollutant limit values recommended by the World Health Organization (WHO)

Air pollution parameter	WHO Limit value (Annual mean)
$PM_{2.5}$	10 µg m^{-3}
PM_{10}	20 µg m^{-3}
*SO_2	125 µg m^{-3*}
NO_2	40 µg m^{-3}

*SO_2 of 125 µg m^{-3} as a 24-h average

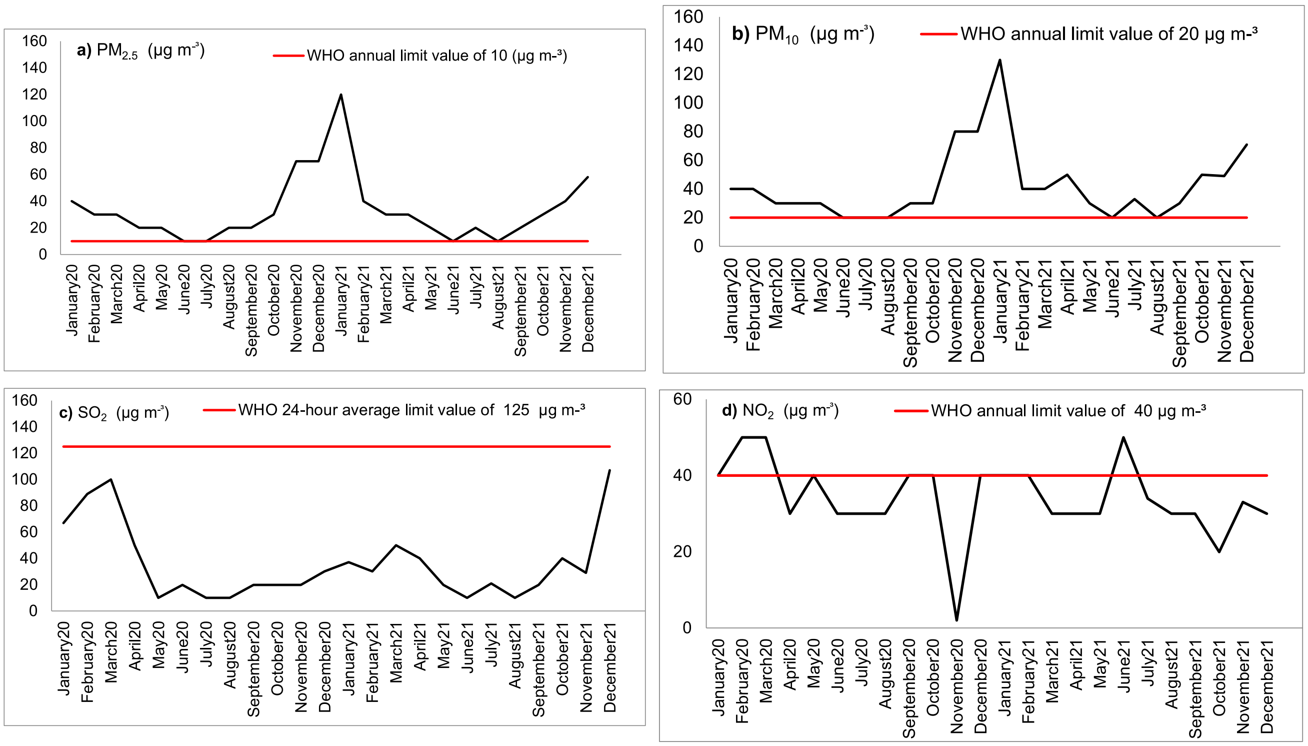

Fig. 3 Graphs showing the monthly variations of air pollutions (**a**) $PM_{2.5}$, (**b**) PM_{10}, (**c**) SO_2, and (**d**) NO_2, from the year 2020 to 2021. The red line shows the limit values of air pollutants given by the World Health Organization

in Italy (57.94 µg m^{-3}), (Aghaei et al. 2024), Pakistan (51.78 µg m^{-3}) and China (75–100 µg m^{-3}) (Li et al. 2022).

The lowest PM_{10} concentrations were recorded in June, July, and August 2020 (20 µg m^{-3}) and in June and August 2021 (20 µg m^{-3}). The highest PM_{10} concentration was 130 µg m^{-3} in January 2021 and 80 µg m^{-3} in November and December 2020 (Fig. 3b). In both years, the PM_{10} concentration was high in the autumn and winter, and lowest in the summer (especially in June). The annual mean PM_{10} was 37.5 µg m^{-3} in 2020 and 46.9 µg m^{-3} in 2021. According to the World Health Organization (2021), the annual average limit value for PM_{10} concentration is 20 µg m^{-3} (Table 3). Correspondingly, the averages in 2020 and 2021 exceeded the limit value and are about 1.9 and 2.3 times higher than this limit value (Fig. 3b). However, the average $PM_{2.5}$ and PM_{10} concentrations in the autumn and winter months of 2020 were 58.33 µg m^{-3} and 65 µg m^{-3}, respectively. In this context, it is suggested that low temperatures may contribute to elevated pollutant levels in the atmosphere. Increased concentrations of particulate matter, originating from emission sources such as vehicles, chimneys, and industrial facilities, are likely to have a negative impact on air quality. Anthropogenic factors such as vehicular traffic and industrial activities effectively increase particulate matter in urban environments (Kim et al. 2015). Factors such as the active traffic of approximately 309 thousand vehicles in the city center (Ayan et al. 2021) and dense residential areas (including domestic heating) are thought to cause high levels of particulate matter accumulation. The harmful effects of these particles in the urban environment may be further exacerbated by aggregation of these particles with metals such as Cd, Cr, Cu, Ni, and Pb emitted by anthropogenic activities (Li et al. 2013). In addition, sand and dust storms of different frequency and duration are common in the steppe regions of Kazakhstan and Central Asia (Issanova et al. 2023). These sand and dust storms are thought to be effective in increasing particulate matter in the atmosphere. Chen et al. (2023) reported that dust storms transported from Mongolia to Beijing, the daily average PM_{10} concentrations exceeded 600 µg m^{-3} and have been soaring since 22 March, and the hourly PM_{10} concentrations have increased from 500 µg m^{-3} to 1490 µg m^{-3}, reaching peak concentrations of 1667 µg m^{-3}, classified as a strong dust storm. Similarly, higher levels of particulate pollution have been reported in Middle Eastern countries such as Pakistan and Arabia as a result of desert dust storms (Mukherjee and Agrawal 2017).

Plants are highly effective at capturing atmospheric particles, which can accumulate on their leaves, branches, and stem surfaces or be absorbed through their stomata (Song et al. 2015; Leonard et al. 2016). In this study conducted in Chessmaster Park, Astana, it is possible to say that different conifer species were particularly negatively affected by high concentrations of particulate matter (Fig. 2). This is due to the high potential of evergreen conifers, associated with their hard leaf structure and thick waxy leaf layers (Barwise and Kumar 2020). Particulate matter also has a negative effect on the biochemical parameters of trees, which can slow down the overall growth and development of plants (Rai 2016; Łukowski et al. 2020). In this regard, symptoms such as necrosis, chlorosis, defoliation, and desiccation were observed as a result of PM accumulation in the leaves of *P. abies, B. pendula, P. pungens, Larix* sp., *P. sylvestris,* and *Juniperus* species in Chessmaster Park during the highest concentrations of particulate matter in the fall and winter months (Fig. 2). Similarly, Roy et al. (2024) and Rai (2016) reported that short-term exposure of plants to particulate matter causes symptoms such as necrotic lesions and death of leaves and even the whole plants, while long-term exposure causes symptoms such as dwarfing, yellowing, reduced growth, and chronic damage. Plants exposed to particulate matter can repeatedly accumulate these pollutants in their leaves, directly causing chronic damage (chlorosis) and yield loss (premature leaf death, reduced height growth) (Łukowski et al. 2020).

The highest SO_2 concentrations were recorded in March 2020 (100 µg m^{-3}) and December 2021 (107 µg m^{-3}) (Fig. 3c). The annual average SO_2 concentration was 37.2 µg m^{-3} in 2020 and 34.5 µg m^{-3} in 2021. According to the World Health Organization (2021), the limit value for SO_2 concentration is 125 µg m^{-3} averaged over 24 h. Accordingly, the average values for 2020 and 2021 and the monthly averages are below the limit values (Fig. 3c). The highest NO_2 concentrations were measured in February 2020, March 2020, and June 2021 (50 µg m^{-3}). The annual average NO_2 concentration was 35.2 µg m^{-3} in 2020 and 33.1 µg m^{-3} in 2021. According to the World Health Organization (2021), the annual average limit value for NO_2 concentration limit is 40 µg m^{-3} (Table 3). Although the annual average NO_2 concentrations in Astana remained below the limit values, they were notably high during the winter of 2020 and the summer of 2021 (Fig. 3d). This atmospheric increase is primarily attributed to industrial activities and motor vehicle exhaust emissions (Gasmi et al. 2017). Consequently, it can be concluded that traffic emissions significantly contribute to NO_2 air pollution, as they are a major source of elevated NO_2 concentrations.

In conclusion, the planting of deciduous and evergreen trees is seen to play a vital role in improving urban soil and air quality. Forest trees are highly effective in mitigating air pollution through filtration and absorption, with the ability to remove 75–80% of particulate pollutants, such as dust, from the urban atmosphere. Consequently, the presence and maintenance of trees in urban areas are not only a matter of public health but also contribute to urban comfort and livability. Given the significant carbon sequestration capacity of mature urban trees, it is essential to prioritize the planning of urban parks and the preservation of mature, healthy trees (Rasoolzadeh et al. 2024).

Heavy metal accumulation and species comparison

Variance analysis of heavy metal contents in different tree species growing in three zones of different pollution levels are given in Table 4. Statistically significant differences in Co, Cr, and Al concentrations were observed among *P. pungens*, *P. abies*, and *B. pendula* species in the light pollution zone. *P. abies* leaves had the highest Fe (719.844 mg kg^{-1}) and Al (260.539 mg kg^{-1}) concentrations and the lowest Ag concentration (0.263 mg kg^{-1}). The highest Mn concentration was 157.741 mg kg^{-1}, Cr concentration was 1.787 mg kg^{-1}, Ni concentration was 2.309 mg kg^{-1}, Zn concentration was 481.275 mg kg^{-1}, and Ba concentration was 163.0749 mg kg^{-1} in *B. pendula* leaves. *P. pungens* leaves had the highest concentrations of Li (3.570 mg kg^{-1}), Ag (2.364 mg kg^{-1}), and *B. pendula* leaves had the lowest concentrations of Li (1.451 mg kg^{-1}). *P. sylvestris* leaves had the highest concentration of Co (0.448 mg kg^{-1}) and, the lowest concentration of Ba (5.481 mg kg^{-1}) (Table 4). The results obtained from the study were compared with the normal ranges in terms of total heavy metal concentrations for the plants as shown in Table 2. The concentrations of Co and Ba were statistically significant ($P < 0.05$) in the leaves of tree species exposed to light pollution relatively far from the traffic density (Table 5). Ayan et al. (2021) conducted a study in Janibek Park, Kazakhstan, and found no statistically significant differences among Ni, Pb, Li, Fe, and Zn concentrations on trees of *P. abies, B. pendula*, and *P. sylvestris* species in the area exposed to severe pollution, while a significant difference was found between Cd, Cr, and Co concentrations. Zhai et al. (2016) reported that the concentrations of Cd, Cr, Cu, Zn, and Pb in plant leaves along the G4 and G60 highways in Yuan Province, China, increased with traffic intensity, identifying these metals as the primary pollution factors within the high to very high risk range. Similarly, Pascu et al. (2024), in their assessment of the Bucharest-Pitesti highway, observed that areas with heavy vehicle traffic, particularly those used for loading, unloading, and housing logistic warehouses, exhibited the highest concentrations of toxic metals such as Cd, As, Cu, and Zn, exceeding the established reference values.

Fe concentrations in leaves of *P. pungens, P. abies, B. pendula, Larix* sp., *Juniperus* sp., and *P. sylvestris* were generally low in the moderate pollution zone ($P < 0.01$, Table 4). When compared with the normal ranges of total heavy metal concentrations for plants, as presented in Table 2, the Fe concentrations were found to be significantly below the normal values. When evaluated under varying pollution levels influenced by traffic density, chlorosis was identified as the

Table 4 Variance analysis of heavy metal concentrations in tree species across three pollution zones (mg kg^{-1})

High Pollution						
Species	Fe	Mn	Cr	Co	Ni	Pb
Picea pungens	277.888 ± 0.277 a	23.215 ± 0.042 b	1.048 ± 0.001 a	0.236 ± 0.011 a	0.943 ± 0.011 b	0.782 ± 0.068 b
Picea abies	719.844 ± 182.211 a	42.243 ± 6.719 ab	1.695 ± 0.189 a	0.311 ± 0.028 a	1.070 ± 0.059 ab	1.367 ± 0.039 a
Betula pendula	378.682 ± 10.529 a	73.843 ± 34.304 a	1.361 ± 0.054 a	0.301 ± 0.009 a	1.279 ± 0.057 a	1.022 ± 0.086 b
F Values. P Level	*1.939–0.163 ns*	*5.785–0.008***	*2.425–0.107 ns*	*1.074–0.356 ns*	*4.943–0.015**	*13.314–0.000****
Species	Al	Ba	Cd	Li	Ag	Zn
Picea pungens	155.813 ± 0.943 a	82.212 ± 0.126 a	0.134 ± 0.002 a	3.570 ± 0.122 a	2.364 ± 0.193 a	56.381 ± 0.119 a
Picea abies	260.539 ± 31.315 a	66.712 ± 6.339 a	0.109 ± 0.008 a	2.119 ± 0.207 a	1.298 ± 0.289 a	55.454 ± 4.386 a
Betula pendula	228.868 ± 5.939 a	61.166 ± 14.374 a	0.137 ± 0.006 a	2.748 ± 0.376 a	1.189 ± 0.269 a	84.339 ± 13.974 a
F Values. P Level	*1.851–0.176 ns*	*0.407–0.670 ns*	*4495–0.061 ns*	*3.095–0.062 ns*	*1.696–0.202 ns*	*2.692–0.086 ns*
Moderate Pollution						
Species	Fe	Mn	Cr	Co	Ni	Pb
Picea pungens	113.864 ± 18.257 b	26.290 ± 0.309 bc	0.531 ± 0.032 c	0.134 ± 0.002 c	0.652 ± 0.096 c	0.871 ± 0.035 d
Picea abies	244.511 ± 19.738 ab	24.897 ± 3.839 bc	1.357 ± 0.163 ab	0.244 ± 0.024 bc	1.170 ± 0.165 bc	1.994 ± 0.107 c
Betula pendula	314.138 ± 17.346 a	157.741 ± 15.183 a	1.787 ± 0.149 a	0.367 ± 0.009 ab	2.309 ± 0.397 a	3.123 ± 0.779 b
Larix sp.	360.053 ± 0.723 a	12.951 ± 0.035 c	1.518 ± 0.006 ab	0.254 ± 0.005 bc	1.027 ± 0.009 bc	1.551 ± 0.049 cd
Juniperus sp.	142.055 ± 2.014 b	41.023 ± 0.449 b	0.839 ± 0.013 bc	0.386 ± 0.011 a	1.158 ± 0.033 bc	6.547 ± 0.124 a
Pinus sylvestris	233.012 ± 54.509 ab	26.793 ± 0.561 bc	1.362 ± 0.131 ab	0.449 ± 0.045 a	1.819 ± 0.056 ab	1.917 ± 0.042 c
F Values. P Level	*4.244–0.003***	*59.242–0.000****	*3.754–0.007***	*10.547–0.000****	*5.789–0.000****	*27.176–0.000****
Species	Al	Ba	Cd	Li	Ag	Zn
Picea pungens	77.513 ± 15.427 c	35.159 ± 3.863 b	0.098 ± 0.015 d	2.902 ± 0.029 b	1.457 ± 0.652 bc	56.692 ± 3.552 b
Picea abies	180.781 ± 16.958 ab	102.108 ± 10.106 a	0.209 ± 0.022 bc	2.686 ± 0.223 b	1.857 ± 0.316 b	77.690 ± 5.736 b
Betula pendula	248.683 ± 16.985 a	103.203 ± 3.950 a	0.299 ± 0.023 b	2.628 ± 0.342 b	1.833 ± 0.213 b	481.275 ± 183.950 a
Larix sp.	248.397 ± 0.576 a	90.925 ± 0.263 a	0.134 ± 0.001 cd	2.399 ± 0.033 b	1.759 ± 0.257 b	46.495 ± 0.091 b
Juniperus sp.	107.042 ± 1.375 c	18.915 ± 0.027 b	0.394 ± .000 a	0.000 ± 0.000 c	0.000 ± 0.000 c	82.460 ± 0.916 b
Pinus sylvestris	181.710 ± 52.991 ab	5.481 ± 0.603 b	0.293 ± 0.00 b	6.442 ± 0.241 a	6.598 ± 0.284 a	47.382 ± 7.778 b
F Values. P Level	*4.072–0.004***	*15.741–0.000****	*10.629–0.000****	*39.801–0.000****	*25.488–0.000****	*7.415–0.000****
Light Pollution						
Species	Fe	Mn	Cr	Co	Ni	Pb
Picea pungens	196.178 ± 25.277 a	42.374 ± 1.659 b	0.818 ± 0.089 b	0.154 ± 0.019 b	0.742 ± 0.058 b	0.977 ± 0.205 a
Picea abies	273.741 ± 29.974 a	14.052 ± 1.127 c	1.162 ± 0.079 a	0.243 ± 0.026 a	0.964 ± 0.211 ab	2.339 ± 0.621 a
Betula pendula	261.810 ± 10.000 a	126.746 ± 13.219 a	1.089 ± 0.023 a	0.256 ± 0.020 a	1.529 ± 0.085 a	1.765 ± 0.172 a
F Values. P Level	*1.860–0.180 ns*	*97.841–0.000****	*4.654–0.021**	*3.805–0.039**	*3.444–0.005***	*1.480–0.250 ns*
Species	Al	Ba	Cd	Li	Ag	Zn
Picea pungens	116.338 ± 14.722 b	87.383 ± 10.523 b	0.096 ± 0.019 a	2.155 ± 0.436 a	0.963 ± 0.269 a	68.272 ± 15.262 b
Picea abies	192.861 ± 17.368 a	118.657 ± 12.091 b	0.169 ± 0.032 a	2.505 ± 0.654 a	0.263 ± 0.994 a	79.850 ± 10.654 b
Betula pendula	195.781 ± 6.382 a	163.075 ± 15.021 a	0.211 ± 0.015 a	1.452 ± 0.110 a	1.523 ± 0.080 a	197.488 ± 15.261 a
F Values. P Level	*5.976–0.009***	*6.234–0.007***	*2.833–0.081 ns*	*0.745–0.487 ns*	*0.989–0.389 ns*	*11.416–0.000****

Heavy metal values (mg kg^{-1}) represent the mean ± standard error (SE). *In cases where the letters in the superscript are different, the data differ significantly (*$*P < 0.05$, $**P < 0.01$, $***P < 0.001$, ns: non-significant*). Fe: Iron, Mn: Manganese, Cr: Chromium, Co: Cobalt, Ni: Nickel, Pb: Lead, Al: Aluminium, Ba: Barium, Cd: Cadmium, Li: Lithium, Ag: Silver, Zn: Zinc

most prevalent condition caused by iron deficiency in plants (Horuz et al. 2016). Factors contributing to iron deficiency primarily prevent the uptake of available iron from the soil by the roots, as well as its transport and metabolism within the plant. Soluble Ca^{++}, HCO_3-, CO_2, and P concentrations are known to play a significant role in the development of iron chlorosis in plants (Shalau 2010; Horuz et al. 2016). In this study conducted in Chessmaster Park in Astana, yellowing of leaves (chlorosis) was commonly observed in the

Table 5 Variance analysis and Newman–Keuls multiple test results of heavy metal concentrations in three pollution zones (mg kg^{-1})

Pollution intensity	Fe	Mn	Cr	Co
High	539.183 ± 95.834 a	52.980 ± 6.068 a	1.497 ± 0.104 a	0.299 ± 0.015 a
Moderate	235.543 ± 16.267 b	47.432 ± 6.846 a	1.286 ± 0.092 ab	0.294 ± 0.019 a
Light	251.367 ± 17.325 b	49.306 ± 10.133 a	1.058 ± 0.053 b	0.224 ± 0.017 b
F Values. P Level	*F:10.684 P:0.000******	*F:0.576 P:0.564 ns*	*F:4.276 P:0.017**	*F:3.912 P:0.023**
Pollution intensity	Ni	Pb	Al	Ba
High	1.141 ± 0.044 a	1.171 ± 0.055 b	237.398 ± 16.591 a	66.044 ± 6.503 b
Moderate	1.360 ± 0.112 a	2.237 ± 0.209 a	176.152 ± 12.799 b	69.860 ± 7.473 b
Light	1.050 ± 0.122 a	1.854 ± 0.331 a	174.460 ± 11.625 b	121.942 ± 9.211a
F Values. P Level	*F:2.370 P:0.099 ns*	*F:6.436 P:0.002***	*F:5.861 P:0.004***	*F:12.492 P:0.000****
Pollution intensity	Cd	Li	Ag	Zn
High	0.122 ± 0.005 b	2.516 ± 0.198 ab	1.361 ± 0.188 b	67.101 ± 6.411 a
Moderate	0.230 ± 0.015 a	3.224 ± 0.269 a	2.571 ± 0.334 a	118.179 ± 29.371 a
Light	0.161 ± 0.019 b	2.154 ± 0.349 b	1.937 ± 0.513 ab	106.365 ± 15.260 a
F Values. P Level	*F:15.306 P:0.000****	*F:3.912 P:0.023**	*F:3.189 P:0.045**	*F:1.156 P:0.319 ns*

Heavy metal values (mg kg^{-1}) represent the mean ± standard error (SE). *In cases where the letters in the superscript are different, the data differ significantly (*$P<0.05$, **$P<0.01$, ***$P<0.001$, *ns: non-significant*). Fe: Iron, Mn: Manganese, Cr: Chromium, Co: Cobalt, Ni: Nickel, Pb: Lead, Al: Aluminium, Ba: Barium, Cd: Cadmium, Li: Lithium, Ag: Silver, Zn: Zinc

majority of tree species, which was attributed to low Fe concentrations (Fig. 2).

Cd concentration was higher in *B. pendula* species than in *P. sylvestris* and *P. abies*, while Cr and Co concentrations were higher in *P. abies* species than in *B. pendula* and *P. sylvestris*. Aydın and Pakyürek (2020) reported that Cd and Pb concentrations in leaf samples did not linearly change depending on the distance to the road (0, 50 and 100 m). Savacı and Öksüz (2020) also emphasized that the accumulation of heavy metals varies significantly depending on the distance from the pollution source.

Mn is the second most abundant trace element in the Earth's crust after Fe and is widely distributed in soils, sediments, and other biological materials (Geszvain et al. 2012). Mn concentrations showed statistically significant differences among all tree species (Table 4). While the Mn concentration was highest in *B. pendula* leaves in the area exposed to moderate pollution (157.741 mg kg^{-1}), it was lowest in *Larix* sp. leaves (12.951 mg kg^{-1}). Excessive Mn concentrations can cause effects (Huang et al. 2018). Mn toxicity causes toxic symptoms such as chlorosis in young leaves, necrotic dark spots on mature leaves, and wrinkled leaves, ultimately inhibit plant growth (Li et al. 2019). Symptoms such as chlorosis and necrosis were also observed in *B. pendula* leaves in Chessmaster Park due to Mn toxicity (Fig. 2). In addition, Mn concentrations in *P. abies* leaves exposed to light pollution were slightly below the limit value (14.051 mg kg^{-1}) and were normal values in other areas.

Zn concentrations in *B. pendula* leaves were quite high in light and moderate pollution areas, while Zn concentrations in *P. abies* and *P. pungens* leaves were normal (Table 6). Similarly, Krupnova et al. (2021) found extremely high concentrations of Zn (316–4000 mg kg^{-1}) in *B. pendula* leaves in Chelyabinsk, Russia, and attributed this increase in concentration to traffic as a source of Zn in the urban environment. Savacı et al. (2024) stated that Zn concentrations in the leaves of *A. negunda*, *A. pseudoplatanus*, and *A. platanoides* were below the limit values, ranging from 10.2 mg kg^{-1} to 34.1 mg kg^{-1}. Therefore, the accumulation of heavy metals may differ among different tree species, especially under the influence of urban pollution.

Pb concentrations in *B. pendula* (3.122 mg kg^{-1}) and *Juniperus* sp. (6.547 mg kg^{-1}) species at moderate pollution intensity were much higher than the limit values and had toxic effects (Table 4). In this study, the highest Pb concentration was found in *Juniperus* leaves. Ayan et al. (2021) conducted a study in Janibek Park in Kazakhstan and found that *B. pendula* species (4.984 mg kg^{-1}) was exposed to the highest Pb concentration due to its large leaf surfaces. Pleijel et al. (2023) found that there was a steady decrease in Pb pollution in *Picea abies* L. on the side of a high-traffic highway with increasing distance from the motorway. While the concentration of Pb was higher than 100 mg kg^{-1} in the samples taken at 15 m from the road, it was revealed that the pollution was higher in the branches in the area of the plant closest to the road than in the branches in the farthest area. Pleijel et al (2023) reported that the change in the concentration of Pb in leaf samples taken from different plants in different regions near the roads in the city of Gothenburg and that there was a positive relationship between the intensity of Pb pollution and the amount of accumulation. Fakayode and Olu-Owalabi (2003) confirmed the positive relationship between Pb concentrations and traffic density. While the Pb concentration in *P.pungens* and *P. abies* species in

Table 6 Variance analysis of heavy metal concentrations in three pollution zones for *Picea abies*, *Betula pendula*, and *Picea pungens* (mg kg^{-1})

Pollution intensity					
Species	*Elements*	*High*	*Moderate*	*Light*	*F Values-P Level*
Picea pungens	Fe	277.888 ± 0.277 a	113.846 ± 18.257 c	196.178 ± 25.276 b	11.63–0.002**
	Mn	23.214 ± 0.042 b	26.290 ± 0.308 b	42.374 ± 1.659 a	75.319- 0.00***
	Cr	1.047 ± 0.001 a	0.531 ± 0.031 c	0.817 ± 0.089 b	12.836–0.001**
	Co	0.236 ± 0.011 a	0.133 ± 0.002 b	0.153 ± 0.019 b	10.078–0.003**
	Ni	0.942 ± 0.010 a	0.652 ± 0.096 a	0.742 ± 0.057 a	2.665–0.110 ns
	Pb	0.781 ± 0.067 a	0.871 ± 0.035 a	0.977 ± 0.204 a	0.373–0.696 ns
	Al	155.813 ± 0.942 a	77.512 ± 15.426 b	15.426 ± 14.721 ab	5.647–0.019*
	Ba	82.211 ± 0.125 a	35.159 ± 3.862 b	87.382 ± 10.522 a	14.698–0.001**
	Cd	0.133 ± 0.001 a	0.098 ± 0.014 a	0.095 ± 0.018 a	1.112–0.360 ns
	Li	3.570 ± 0.122 a	2.901 ± 0.029 ab	2.154 ± 0.436 b	4.398–0.037*
	Ag	2.364 ± 0.192 a	1.456 ± 0.651 a	0.963 ± 0.268 a	1.556–0.251 ns
	Zn	56.381 ± 0.119 a	56.691 ± 3.552 a	68.272 ± 15.261 a	0.400–0.679 ns
Picea abies	*Elements*	*High*	*Moderate*	*Light*	*F Values- P Level*
	Fe	719.844 ± 182.21 a	244.511 ± 19.738 b	273.740 ± 29.973 b	6.927–0.002**
	Mn	42.242 ± 6.719 a	24.897 ± 3.838 b	14.051 ± 1.126 b	7.915–0.001**
	Cr	1.695 ± 0.189 a	1.356 ± 0.162 a	1.162 ± 0.079 a	2.327–0.109 ns
	Co	0.310 ± 0.002 a	0.244 ± 0.023 a	0.242 ± 0.025 a	2.131–0.131 ns
	Ni	1.070 ± 0.058 a	1.170 ± 0.165 a	0.963 ± 0.211 a	0.413–0.664 ns
	Pb	1.366 ± 0.038 a	1.993 ± 0.106 a	0.233 ± 0.621 a	2.711–0.077
	Al	260.539 ± 0.313 a	180.781 ± 16.958 b	192.861 ± 17.368 b	3.664–0.034*
	Ba	66.712 ± 6.339 b	102.107 ± 10.106 a	118.657 ± 12.090 a	6.300–0.004**
	Cd	0.108 ± 0.007 b	0.209 ± 0.022 a	0.169 ± 0.031 ab	5.722–0.006**
	Li	2.119 ± 0.206 a	2.685 ± 0.222 a	2.505 ± 0.654 a	0.740–0.483 ns
	Ag	1.298 ± 0.288 a	1.857 ± 0.316 a	2.631 ± 0.994 a	1.405–0.256 ns
	Zn	55.454 ± 4.285 b	77.689 ± 5.735 a	79.849 ± 10.653 a	3.769–0.031*
Betula pendula	*Elements*	*High*	*Moderate*	*Light*	*F Values- P Level*
	Fe	378.682 ± 10.529 a	314.138 ± 17.346 b	261.810 ± 10.000 c	22.678–0.000***
	Mn	73.842 ± 9.902 a	157.740 ± 15.182 b	126.745 ± 13.219 b	12.947–0.000***
	Cr	1.360 ± 0.053 b	1.787 ± 0.149 a	1.088 ± 0.023 c	14.736–0.000***
	Co	0.301 ± 0.008 b	0.366 ± 0.008 a	0.255 ± 0.020 c	16.125–0.000***
	Ni	1.279 ± 0.057 b	2.309 ± 0.397 a	1.529 ± 0.085 b	8.345–0.002**
	Pb	1.022 ± 0.085 b	3.122 ± 0.778 a	1.764 ± 0.171 b	9.254–0.001**
	Al	228.868 ± 5.939 a	24.868 ± 16.984 a	195.780 ± 6.381 b	6.257–0.007**
	Ba	61.166 ± 14.373 b	103.202 ± 3.950 b	163.074 ± 15.021 a	12.729–0.000***
	Cd	0.136 ± 0.005 c	0.298 ± 0.022 a	0.210 ± 0.014 b	43.025–0.000***
	Li	2.747 ± 0.375 a	2.627 ± 0.341 a	1.451 ± 0.110 a	3.343–0.055 ns
	Ag	1.188 ± 0.269 a	1.832 ± 0.212 a	1.523 ± 0.080 a	1.620–0.222 ns
	Zn	84.339 ± 13.974 b	481.274 ± 183.949 a	197.488 ± 36.341b	6.140–0.008

Heavy metal values (mg kg^{-1}) represent the mean ± standard error (SE). *In cases where the letters in the superscript are different, the data differ significantly (*$P < 0.05$, **$P < 0.01$, ***$P < 0.001$, *ns: non-significant*). Fe: Iron,

Mn: Manganese, Cr: Chromium, Co: Cobalt, Ni: Nickel, Pb: Lead, Al: Aluminium, Ba: Barium, Cd: Cadmium, Li: Lithium, Ag: Silver, Zn: Zinc

areas exposed to three different pollution levels was normal, the Pb concentration in *B. pendula* leaves with moderate pollution slightly exceeded the limit value (3.12 mg kg^{-1}).

Ag is a heavy metal that enters from natural and anthropogenic sources (photo-processing wastewater, sewage sludge, etc.) and is not essential for any living organism. However, there are very few data on the toxicity of Ag in plants (Hajar et al. 2014). Ag content in plants should generally be less than 0.01 mg kg^{-1} (Kabata-Pendias and Pendias 2001). However, in this study conducted in Chessmaster Park, Ag concentrations were surprisingly high in the leaves of all tree species at different distances from traffic density (Table 4). The most likely reason for tree roots entering sewer systems or storm drains in urban parks is to access water and nutrients (Fransson 2019). Fransson (2019) stated in his study that the high Ag concentration in the leaves of the trees increased because the roots of the trees entered the sewer pipe. Ndlovu et al. (2025) have stated that nanosilver and ionic silver can be released from textiles into wash water and end up in municipal wastewater. Also, due to the increased use of silver as a disinfectant in sportswear in recent years, nanosilver released during washing and showering can be transported into the sewage system (Fransson 2019). Additionally, the potential for silver toxicity in plants may be attributable to the proximity of the Foto Express shop (190 m) and the large Kacca shopping center (250 m) to the park. The major component of photographic film is composed of silver halide salts: silver chloride, silver bromide, and silver iodide (Calixto et al. 2018). Silver in the photography industry can accumulate to a greater extent in urban soils than rural soils (Andersson and Ladenberger 2010). However, it has been observed in the literature that the environmental effects of Ag toxicity in soil and plants have been studied much less than other heavy metals such as Cr, Zn, and Ni. Ag toxicity in soils and plants is usually caused by anthropogenic pollution, such as gases emitted by thermal power plants during coal combustion, iron alloy metallurgical enterprises, cement factories, solid waste landfills, production of photographic and electrical materials, pesticides, use of sewage sludge as fertilizer (Kolesnikov et al. 2020).

The mean of pollution intensity in different areas according to pollution intensity are given in Table 5. Variations in foliar concentrations of Fe, Cr, Co, Pb, Al, Ba, Cd, Li, and Ag averaged over all species in each zone were statistically significant ($P < 0.05$) in different pollution intensities. While the concentrations of Fe (539.183 mg kg^{-1}), Cr (1.496 mg kg^{-1}), Co (0.299 mg kg^{-1}), and Al (237.398 mg kg^{-1}) were the highest in the leaves in high pollution, Pb (2.236 mg kg^{-1}), Cd (0.229 mg kg^{-1}), Li (3.223 mg kg^{-1}), and Ag (2.571 mg kg^{-1}) concentrations were the lowest in leaves under moderate pollution. Concentrations of Fe, Al, and Ba were below the limit values and were quite low in low and moderate pollution plots; Ag concentration was far above the limit value, and Cr, Co, Pb, Cd, and Li concentrations were within the normal range in all pollution plots (Table 5). Differences in heavy metal concentrations between areas (light, moderate, and high pollution) according to their distance from the pollution source based on tree species are given in Table 6. These three tree species are evaluated because only *P. pungens, P. abies*, and *B. pendula* species are included in the areas exposed to three different pollution intensities. Other tree species are not listed in Table 6 because they are only present at moderate pollutions. There are statistically significant differences in Fe ($P = 0.002$), Mn ($P = 0.00$), Cr ($P = 0.001$), Co ($P = 0.003$), Al ($P = 0.019$), Ba ($P = 0.001$), and Li ($P = 0.037$) concentrations in *P. pungens* according to pollution intensity. There are statistically significant differences in Fe ($P = 0.002$), Mn ($P = 0.001$), Al ($P = 0.034$), Ba ($P = 0.004$), Cd ($P = 0.006$), and Zn ($P = 0.031$) concentrations in *P. abies* leaves according to pollution intensity. There is a statistically significant differences for all heavy metal concentrations in *B. pendula* species, except for Li and Ag. Due to the decrease in pollution intensity, it is observed that Al, Cd, Li, and Ag concentrations decreased in *P. pungens* leaves, Mn, Cr, Co concentrations decreased in *P. abies* leaves, and Fe and Li concentrations decreased in *B. pendula* leaves (Table 6).

Conclusion

This study examined the effects of air pollutants and heavy metal accumulation on six forest tree species (*P. pungens, P. abies, B. pendula, Juniperus* sp., *Larix* sp., and *P. sylvestris*) in Chessmaster Park, Astana. The findings revealed that heavy metal accumulation in tree leaves varied depending on their proximity to traffic density. Deficiencies of iron (Fe) and aluminum (Al), as well as silver (Ag) toxicity, were observed in the leaves of all tree species analyzed. Among the species, *B. pendula* exhibited the highest accumulation of heavy metals, particularly manganese (Mn), zinc (Zn), and lead (Pb). The results underscore that dense urban living conditions, characterized by high air pollutant levels, exacerbate the impact of heavy metal pollution on plants. Anthropogenic factors, including motor vehicle exhaust emissions, dust transport, wastewater (sewage), and domestic heating associated with traffic density, were found to adversely affect the growth and development of forest trees in Chessmaster Park.

In the context of Astana's harsh continental climate and high traffic-related pollution, the selection of tree species for urban parks should balance climatic resilience, pollutant filtration capacity, and species diversity. Conifers such as *Picea pungens*, *Pinus sylvestris*, and *Juniperus* spp. are highly suitable along main roads, as their evergreen needle foliage provides year-round interception of particulate matter and heavy metals (e.g., Pb, Cd, Zn). Among deciduous species, *Betula pendula* and *Tilia cordata* exhibit strong tolerance and accumulation capacity for Zn, Mn, and Pb, while *Acer platanoides* and *Ulmus pumila* combine heavy metal resilience with adaptability to Astana's cold and dry winters. Incorporating a mixture of coniferous and broadleaf trees not only enhances pollutant capture across different seasons but also strengthens the ecological stability and visual quality of urban green spaces. Thus, a diversified planting scheme using these species can effectively mitigate heavy metal pollution while ensuring long-term functionality and sustainability of Astana's urban parks. This study provides valuable insights into the relationship between urban pollution and heavy metal accumulation in plants, offering a foundation for future research to better understand how plants tolerate the toxicity of different heavy metals in urban environments.

Acknowledgements The authors express their gratitude to the Kazhydromet Station for providing the air quality parameter data utilized in this study.

Author contributions All authors contributed to the study's conception and design. The authors indicated in parentheses made substantial contributions to the following tasks of research: Sezgin Ayan: Investigation; Methodology; Data curation; Statistical analysis; Visualization; Writing—original draft. Dani Sarsekova: Data curation; Methodology; Resources; Visualization; Gani Kenesaryuly: Data curation; Methodology; Resources; Visualization; Gamze Savacı: Visualization; Resources; Writing—original draft; Orhan Gülseven: Statistical analysis; Validation; Visualization; Ergin Yılmaz & Şeyma Selin Akın: Lab analysis; Validation; Visualization. All authors read and approved the final manuscript.

Funding This study was conducted without any financial support or external funding.

Data availability Not applicable.

Declarations

Conflict of interest The authors declare no confict of interest.

Ethical approval This article does not involve any studies conducted with human participants or animals by the authors.

References

Abdel-Sabour MF, Rabie FH (2003) Accumulation of heavy metals in vegetable plants grown in mostorod area. Egypt J Soil Sci 43:63–76

Aghaei Y et al (2024) The impact of Russia-Ukraine geopolitical conflict on the air quality and toxicological properties of ambient $PM_{2.5}$ in Milan, Italy. Sci Rep 14(1):5996. https://doi.org/10.1038/s41598-024-55292-2

Almaganbetovna TA et al (2023) Development of the architecture of residential buildings from the beginning of XX to XXI century (by the example of Astana). Civ Eng Archit 11(3):1220–1233. https://doi.org/10.13189/cea.2023.110308

Andersson M, Ladenberger A (2010) Geokemiska Kartan Markgeokemi - Skåne och tätorterna Malmö, Lund och Helsingborg. Sver Geol Unders K305:1–147

Ayan S et al (2021) Accumulation of heavy metal pollution caused by traffic in forest trees in the Park of Kerey and Janibek Khans of the city of Nur-Sultan. Kazakhstan. J for Sci 67(7):357–366. https://doi.org/10.17221/37/2021-JFS

Aydın ŞD, Pakyürek M (2020) Heavy metal accumulation potential in pomegranate fruits and leaves grown in roadside orchards. PeerJ 8:e8990

Barwise Y, Kumar P (2020) Designing vegetation barriers for urban air pollution abatement: a practical review for appropriate plant species selection. NPJ Clim Atmos Sci 3(1):12. https://doi.org/10.1038/s41612-020-0115-3

Bolan N, Hoang SA, Tanveer M, Wang L, Bolan S, Sooriyakumar P, Robinson B, Wijesekara H, Wijesooriya M, Keerthanan S, Vithanage M, Markert B, Fränzle S, Wünschmann S, Sarkar B, Vinu A, Kirkham MB, Siddique KHM, Rinklebe J (2021) From mine to mind and mobiles–Lithium contamination and its risk management. Environ Pollut 290:118067

BUREAU of National Statistics (2025) *Population statistics*. Retrieved from https://stat.gov.kz/ Accessed on 19.02.2025.

Calixto S et al (2018) Gelatin as a photosensitive material. Molecules 23(8):2064. https://doi.org/10.3390/molecules23082064

Chen S et al (2023) Mongolia contributed more than 42% of the dust concentrations in Northern China in March and April 2023. Adv Atmos Sci 40:1549–1557. https://doi.org/10.1007/s00376-023-3062-1

Codex (2003) Alimentarius commission. Maximum levels for lead codex standard 230-2001, Rev. 1-2003

Costa LG et al (2019) Developmental impact of air pollution on brain function. Neurochem Int 131:104580. https://doi.org/10.1016/j.neuint.2019.104580

Coulon F et al (2016) China's soil and groundwater management challenges: lessons from the UK's experience and opportunities for China. Environ Int 91:196–200. https://doi.org/10.1016/j.envint.2016.02.023

Dao L et al (2014) Influences of traffic on Pb, Cu and Zn concentrations in roadside soils of an urban park in Dublin, Ireland. Environ Geochem Health 36:333–343. https://doi.org/10.1007/s10653-013-9553-8

Fakayode SO, Olu-Owolabi BI (2003) Heavy metal contamination of roadside topsoil in Osogbo, Nigeria: its relationship to traffic density and proximity to highways. Environ Geol 44(2):150–157. https://doi.org/10.1007/s00254-002-0739-0

FAO O (2014) Proposed draft maximum levels for cadmium in chocolate and cocoa-derived products. Programa Conjunto FAO/OMS sobre normas alimentarias comisión del codex sobre contaminación en los alimentos 6:1–20

Fransson AM (2019) Can silver and other heavy metal concentrations in leaves be used in order to identify tree root intrusion into sewage systems and storm-water drains? Arboric J 41(4):212–225. https://doi.org/10.1080/03071375.2019.1677418

Gasmi K et al (2017) Analysis of NOx, NO and NO_2 ambient levels as a function of meteorological parameters in Dhahran, Saudi Arabia. WIT Trans Ecol Environ 211:77–86. https://doi.org/10.2495/AIR170081

Geszvain K et al (2012) The molecular biogeochemistry of manganese (II) oxidation. Biochem Soc Trans 40(6):1244–1248. https://doi.org/10.1042/BST20120229

Ghio AJ et al (2012) Diesel exhaust particles and airway inflammation. Curr Opin Pulm Med 18(2):144–150. https://doi.org/10.1097/MCP.0b013e32834f0e2a

Hajar EWI et al (2014) Assessment of heavy metals tolerance in leaves, stems and flowers of *Stevia rebaudiana* plant. Procedia Environ Sci 20:386–393. https://doi.org/10.1016/j.proenv.2014.03.049

Heidari M et al (2021) Heavy metal pollution of road dust in a city and its highly polluted suburb; quantitative source apportionment and source-specific ecological and health risk assessment.

Chemosphere 273:129656. https://doi.org/10.1016/j.chemosphere.2021.129656

Horuz A et al (2016) Bitkilerde demir klorozunun nedenleri ve giderilme yöntemleri. Toprak Bilimi Ve Bitki Besleme Dergisi 4(1):32–42

Hu Y et al (2014) Bioaccumulation of heavy metals in plant leaves from Yan′ an city of the Loess Plateau, China. Ecotoxicol Environ Saf 110:82–88. https://doi.org/10.1016/j.ecoenv.2014.08.021

Huang H et al (2018) Biosorption characteristics of a highly Mn (II)-resistant *Ralstonia pickettii* strain isolated from Mn ore. PLoS ONE 13(8):e0203285. https://doi.org/10.1371/journal.pone.0203285

Huang J et al (2021) Health risk assessment of heavy metal (loid) s in park soils of the largest megacity in China by using Monte Carlo simulation coupled with Positive matrix factorization model. J Hazard Mater 415:125629. https://doi.org/10.1016/j.jhazmat.2021.125629

Issanova G et al (2023) Spatial and temporal characteristics of dust storms and aeolian processes in the Southern Balkash deserts in Kazakhstan, Central Asia. Land 12(3):668. https://doi.org/10.3390/land12030668

Jansen S, Broadley MR, Robbrecht E, Smets E (2002) Aluminum hyperaccumulation in angiosperms: a review of its phylogenetic significance. Bot Rev 68(2):235–269

Jin S et al (2014) Evaluation of impacts of trees on $PM_{2.5}$ dispersion in urban streets. Atmos Environ 99:277–287. https://doi.org/10.1016/j.atmosenv.2014.10.002

Kabata-Pendias A, Pendias H (1984) Trace elements in soils and plants. CRC Press, Boca Raton, Florida

Kabata-Pendias A, Pendias H (2001) Trace elements in soils and plants. CRC Press, Washington, DC

Kazhydromet (2024) Monthly newsletter on the state of the environment. The link was accessed on 28.04.2024. https://www.kazhydromet.kz/ru/ecology/ezhemesyachnyy-informacionnyy-byulleten-o-sostoyanii-okruzhayuschey-sredy

Kim KH et al (2015) A review on the human health impact of airborne particulate matter. Environ Int 74:136–143. https://doi.org/10.1016/j.envint.2014.10.005

Kolesnikov SI et al (2020) Silver ecotoxicity estimation by the soil state biological indicators. Appl Environ Soil Sci 2020:1–9. https://doi.org/10.1155/2020/1207210

Kończak B et al (2021) Assessment of the ability of roadside vegetation to remove particulate matter from the urban air. Environ Pollut 268:115465. https://doi.org/10.1016/j.envpol.2020.115465

Krupnova TG et al (2021) Extremely high concentrations of zinc in birch tree leaves collected in Chelyabinsk, Russia. Environ Geochem Health 43:2551–2570. https://doi.org/10.1007/s10653-020-00605-3

Kumar A et al (2021) Adaptation and mitigation potential of roadside trees with bio-extraction of heavy metals under vehicular emissions and their impact on physiological traits during seasonal regimes. Urban for Urban Green 58:126900. https://doi.org/10.1016/j.ufug.2020.126900

Kumar MS et al (2025) Assessing heavy metal contamination in roadside soils as a consequence of motor vehicle emissions. Int J Environ Sci Technol 22(8):7119–7132. https://doi.org/10.1007/s13762-024-06118-1

Lavilla I et al (1999) Comparison of digestion methods for determination of trace and minor metals in plant samples. J Agric Food Chem 47(12):5072–5077. https://doi.org/10.1021/jf990336w

Leonard RJ et al (2016) Particulate matter deposition on roadside plants and the importance of leaf trait combinations. Urban for Urban Green 20:249–253. https://doi.org/10.1016/j.ufug.2016.09.008

Li H et al (2013) Heavy metals in atmospheric particulate matter: a comprehensive understanding is needed for monitoring and risk mitigation. Environ Sci Technol 47(23):13210–13211. https://doi.org/10.1021/es404751a

Li J et al (2019) Advances in the mechanisms of plant tolerance to manganese toxicity. Int J Mol Sci 20(20):5096. https://doi.org/10.3390/ijms20205096

Li S et al (2022) $PM_{2.5}$ concentration exposure over the belt and road region from 2000 to 2020. Int J Environ Res Public Health 19(5):2852. https://doi.org/10.3390/ijerph19052852

Łukowski A et al (2020) Particulate matter on foliage of *Betula pendula*, *Quercus robur*, and *Tilia cordata*: deposition and ecophysiology. Environ Sci Pollut Res Int 27(10):10296–10307. https://doi.org/10.1007/s11356-020-07672-0

Matin G et al (2016) Bio-monitoring of cadmium, lead, arsenic and mercury in industrial districts of Izmir, Turkey by using honey bees, propolis and pine tree leaves. Ecol Eng 90:331–335. https://doi.org/10.1016/j.ecoleng.2016.01.035

Misra SG, Mani D (1991) Soil pollution. Ashish Publishing House, Punjabi Bagh

Mukherjee A, Agrawal M (2017) World air particulate matter: sources, distribution and health effects. Environ Chem Lett 15:283–309. https://doi.org/10.1007/s10311-017-0611-9

Nadgórska-Socha A et al (2017) Air pollution tolerance index and heavy metal bioaccumulation in selected plant species from urban biotopes. Chemosphere 183:471–482. https://doi.org/10.1016/j.chemosphere.2017.05.128

Ndlovu LN et al (2025) A review on nanomaterial contaminants and their removal from industrial and municipal wastewater by conventional filtration and ultrafiltration membrane techniques. AIMS Mater Sci 12(2):336–362. https://doi.org/10.3934/matersci.2025018

Orlovsky NS et al (2013) Severe dust storms in Central Asia. Arid Ecosyst 3:227–234. https://doi.org/10.1134/S2079096113040082

Pais I, Jones Jr JB (1997) The handbook of trace elements. Crc Press

Palit S et al (1994) Effects of cobalt on plants. Bot Rev 60:149–181. https://doi.org/10.1007/BF02856575

Pascu LF et al (2024) Spatiotemporal assessment of soil and vegetation pollution with toxic metals from road traffic along the first Romanian highway. Environments 11(1):21. https://doi.org/10.3390/environments11010021

Pleijel H et al (2023) Accumulation of antimony and lead in leaves and needles of trees: the role of traffic emissions. Heliyon. https://doi.org/10.1016/j.heliyon.2023.e13548

Rai PK (2016) Impacts of particulate matter pollution on plants: implications for environmental biomonitoring. Ecotoxicol Environ Saf 129:120–136. https://doi.org/10.1016/j.ecoenv.2016.03.012

Rasoolzadeh R et al (2024) Carbon sequestration and storage of urban trees in a polluted semiarid city. Forests 15(9):1488. https://doi.org/10.3390/f15091488

Roy A et al (2024) The cellular consequences of particulate matter pollutants in plants: safeguarding the harmonious integration of structure and function. Sci Total Environ. https://doi.org/10.1016/j.scitotenv.2023.169763

Savacı G, Öksüz Ç (2020) Investigation of heavy metal concentrations in soil caused by Kastamonu city wild storage dumpsite. Turk J for Sci 4(1):26–39. https://doi.org/10.32328/turkjforsci.703836

Savacı G et al (2024) Effect of drought and soil heavy metal contamination on three maple species: a case study of Kastamonu University campus in Türkiye. Environ Monit Assess 196(1):46. https://doi.org/10.1007/s10661-023-12233-2

Shalau J (2010) Laboratories conducting soil, plant, feed or water testing. Publication AZ1111, College of Agriculture and Life Science, University of Arizona.

Singh H et al (2020) Assessing adaptation and mitigation potential of roadside trees under the influence of vehicular emissions: a case study of *Grevillea robusta* and *Mangifera indica* planted in an urban city of India. PLoS ONE 15(1):e0227380. https://doi.org/10.1371/journal.pone.0227380

Song Y et al (2015) Particulate matter deposited on leaf of five evergreen species in Beijing, China: source identification and size distribution. Atmos Environ 105:53–60. https://doi.org/10.1016/j.atmosenv.2015.01.032

URL1 (2021) http://www.pogodaiklimat.ru/climate/35188.htm (Accessed: April 30, 2021).

Wang L et al (2018) Survey of ecological environmental conditions and influential factors for public parks in Shanghai. Chemosphere 190:9–16. https://doi.org/10.1016/j.chemosphere.2017.09.061

Wang X et al (2022) Traffic emission dominates the spatial variations of metal contamination and ecological-health risks in urban park soil. Chemosphere 297:134155. https://doi.org/10.1016/j.chemosphere.2022.134155

WDB (World Data Bank) (2025) World Development Indicators. available at: https://databank.worldbank.org/databases/page/1/orderby/popularity/direction/desc

World Health Organization (2021) WHO global air quality guidelines: particulate matter ($PM_{2.5}$ and PM_{10}), ozone, nitrogen dioxide, sulfur dioxide and carbon monoxide. World Health Organization.

Zayed AM, Terry N (2003) Chromium in the environment: factors affecting biological remediation. Plant Soil 249:139–156. https://doi.org/10.1023/A:1022504826342

Zhai Y et al (2016) Traffic-related heavy metals uptake by wild plants grow along two main highways in Hunan province, China: effects of soil factors, accumulation ability, and biological indication potential. Environ Sci Pollut Res 23:13368–13377. https://doi.org/10.1007/s11356-016-6507-6

Zhao L et al (2020) Source apportionment and health risks of the bioavailable and residual fractions of heavy metals in the park soils in a coastal city of China using a receptor model combined with Pb isotopes. CATENA 194:104736. https://doi.org/10.1016/j.catena.2020.104736